Journal of Inorganic and General Chemistry
ZAAC
Zeitschrift für anorganische und allgemeine Chemie
DOI: 10.1002/zaac.201900327
ARTICLE

Synthesis, Structure, and Stability of Lithium Arylphosphanidyl-diarylphosphane Oxide

Damian Bevern,[a] Helmar Görls,[a] Sven Krieck,[a] and Matthias Westerhausen*[a]

Dedicated to Professor Dr. Manfred Scheer on the Occasion of his 65th Birthday

Abstract. The reaction of LiP(H)Tipp (**2a**) and KP(H)Tipp (**2b**, Tipp = C_6H_2-2,4,6-*i*Pr_3), which are accessible via metalation of Tipp-PH_2 (**1**), with bis(4-*tert*-butylphenyl)phosphinic chloride yields Tipp-P=P(OM)Ar_2 [M = Li (**3a**) and K (**3b**)]. These complexes show characteristic chemical ^{31}P shifts and large $^{1}J_{PP}$ coupling constants. These compounds degrade with elimination of the phosphinidene Tipp-P: and the alkali metal diarylphosphinites M–O–PAr_2 [M = Li (**4a**) and K (**4b**)]. The phosphinidene forms secondary degradation products (like the *meso* and *R*,*R*/*S*,*S*-isomers of diphosphane Tipp-P(H)–P(H)Tipp (**5**) via insertion into a P–H bond of newly formed Tipp-PH_2), whereas the crystallization of [Tipp-P=P(OLi)Ar_2·LiOPAr_2·LiCl·$2Et_2O$]$_2$ (i.e. [**3a·4a**·LiCl·$2Et_2O$]$_2$) succeeds from diethyl ether. The metathesis reactions of LiP(Si*i*Pr_3)Tipp and LiP(Si*i*Pr_3)Mes (Mes = C_6H_2-2,4,6-Me_3) with Ar_2P(O)Cl yield Ar*-P=P(OSi*i*Pr_3)Ar_2 (Ar* = Mes, Tipp) which degrade to Ar_2POSi*i*Pr_3 and other secondary products.

Introduction

Phosphorus and carbon are often considered being copies of each other, based on very similar reactivity due to the diagonal relationship in the periodic Table and based on comparable electronegativity values [Allred-Rochow electronegativity: EN(C) = 2.50, EN(P) = 2.06] leading to similar bond polarity.[1] This analogy is significantly more expressed than the similitudes within the homologous N/P pair due to a larger electronegativity difference [EN(N) = 3.07]. In Scheme 1, the isoelectronic compounds of the type Ar_2P(O)–ER [E = CH_2 (**A**), NH (**B**), O (**C**)] are depicted; homologous congeners are marked with an apostrophe. Phosphane oxides **A** are stable compounds, whereas it has been known for many years[2] that silyl congeners rearrange yielding siloxy-diarylphosphanes **A′**, which often are now commercially available. The amino-diarylphosphane oxides **B** represent a widely used substance class.[3] Substituted diphosphane monoxides **B'** are also easily prepared[4] and gained academic interest due to unexpected reactivity.[5] The equilibrium between diphosphane monoxides R_2P–P(O)R_2 and anhydrides of phosphorus acids R_2P–O–PR_2 has already been studied in dependency of the substituents at phosphorus.[6] Tautomeric proton shifts from phosphorus to oxygen have not been observed in ArP(H)–P(O)(H)Ar with bulky aryl groups (Ar = C_6H_3-2,6-Mes_2) and the crystal structure determination gave a P–P single bond length of 219.46(8) pm for this diphosphane monoxide.[7] Organyl diarylphosphinates **C** and *S*-organyl diphenylphosphinothioates **C′** are common compounds in organophosphorus chemistry and therefore often commercially available.[8]

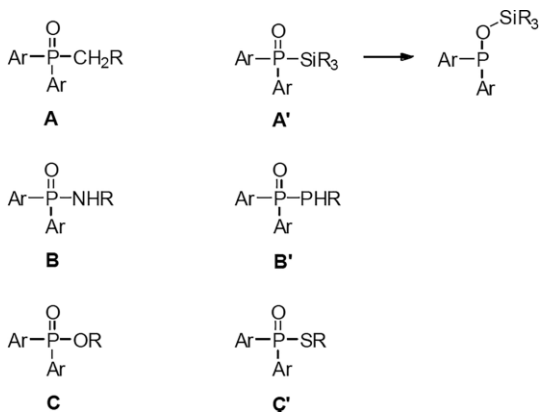

Scheme 1. Isoelectronic compounds of the type Ar_2P(O)-ER with E = CH_2 (**A**), NH (**B**), O (**C**) (left column). The homologous derivatives are marked with an apostrophe (right column). Note that Ar_2P(O)H has a P–H bond, whereas the silyl-substituted congener immediately rearranges to a siloxy phosphane.

Lithiation (deprotonation) of benzyl-diarylphosphane oxides **A**, amino-diarylphosphane oxides **B** and phosphanyl-diarylphosphane oxides **B′** yields compounds with two tautomeric forms as depicted in Scheme 2. More than 40 years ago, lithiated benzyl-diarylphosphane oxides have been prepared and isolated as yellow substances,[9] but in other cases these compounds have been proposed as intermediates.[10]

* Prof. Dr. M. Westerhausen
E-Mail: m.we@uni-jena.de
[a] Friedrich Schiller University Jena
Chair for Inorganic Chemistry 1
Humboldtstraße 8
07743 Jena, Germany
Supporting information for this article is available on the WWW under **http://dx.doi.org/10.1002/zaac.201900327** or from the author.

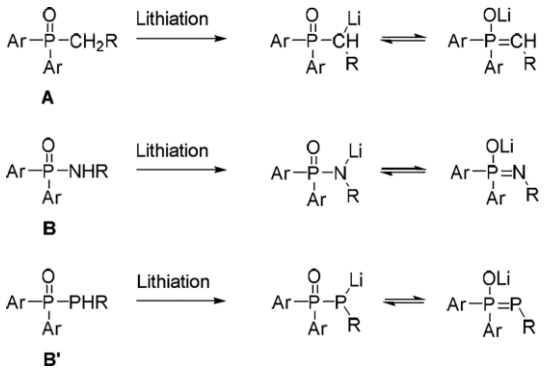

Scheme 2. Lithiation of $Ar_2P(O)$-ER with E = CH_2 (**A**), NH (**B**), P (**B′**) and depiction of the tautomeric forms with O-Li or E–Li bonds.

Lithiation of **B** with n-butyllithium yields lithium amidodiarylphosphane oxides which crystallize from tetrahydrofuran as a dimeric thf adduct with a central eight-membered (Li–N–P–O)$_2$ ring.[11] Homologous derivatives of sodium and potassium have also been prepared using the metals or their amides, alkoxides, and bis(trimethylsilyl)amides.[12]

Lithiated diphosphane monoxides are unknown as of yet. However, early investigations on comparable derivatives show fast degradation. Thus the sodium salt $Ph_2P(O)$–P(Na)–CN has been prepared via the reaction of sodium diphenylphosphinite with [(18-C-6)KP(CN)$_2$] with elimination of a cyanide. The formation of $Ph_2P(O)$–P(Na)-CN [or $Ph_2P(ONa)$=P–CN after migration of the sodium atom] has been verified immediately after the reaction by the characteristic $^{31}P\{^1H\}$ NMR spectrum with two doublets at δ = +55.7 and –161.4 ppm and a $^1J_{PP}$ coupling constant of 362.5 Hz.[13] However, this compound degrades very fast and shortly after the initial spectrum only NaO–PPh_2=P–PPh_2=O has been detected. This complex has also been prepared via the reaction of lithium or sodium diphenylphosphinite with white phosphorus. The structure of the acetonitrile adduct of the lithium derivative with a chelating O–PPh_2=P–PPh_2=O ligand shows two quite equal P–P bond lengths of 212.3(5) and 215.9(5) pm.[14]

The compounds of the types R′$_3$P=ER and $Ar_2P(OM)$=ER can be looked at as phosphane- or phosphinite-stabilized phosphinidenes (E = P), respectively.[15] Phosphinidenes RP: generated in the presence of trialkylphosphane PR'$_3$ can easily be trapped yielding phosphanylidenephosphoranes, R′$_3$P=P–R.[16,17] Furthermore, phosphaalkenes can also act as phosphinidene sources under certain reaction conditions.[18] Another large compound class containing singlet phosphinidene ligands are metal complexes of the type [L_nM=PR], which have been studied extensively; often these complexes are suitable synthons to investigate the chemistry and reactivity of ligated singlet phosphinidenes.[19] In all these compounds singlet phosphinidene moieties have been observed.

The objective of this study was the unequivocal characterization of compounds of the type $Ar_2P(O)$–P(M)–Ar′ to elucidate the nature of the P–P bonding situation. Preliminary experiments showed that the mesityl (Mes = 2,4,6-trimethylphenyl) was not bulky enough to stabilize such complexes. Therefore, we have chosen the 2,4,6-triisopropylphenyl (Tipp) substituent for our investigations to decelerate degradation reactions.

Results and Discussion

Syntheses and Reactivity Studies

Metalation of 2,4,6-triisopropylphenylphosphane (Tipp-PH_2, **1**) with *n*-butyllithium and subsequent recrystallization from a solvent mixture of THF, *n*-hexane and TMEDA yielded quantitatively mononuclear [(thf)(tmeda)Li-P(H)-Tipp] (**2a**, Scheme 3) with a characteristic P–H stretching vibration at 2297 cm^{-1}. Deprotonation of **1** with KH in diethyl ether/THF at 0 °C gave amorphous [(thf) K-P(H)-Tipp]$_\infty$ recrystallization from a mixture of diethyl ether and TMEDA led to substitution of the ligated Lewis base and to crystallization of [(tmeda)$_{0.5}$K-P(H)-Tipp]$_\infty$ (**2b**) with a P–H stretching mode at 2259 cm^{-1}.

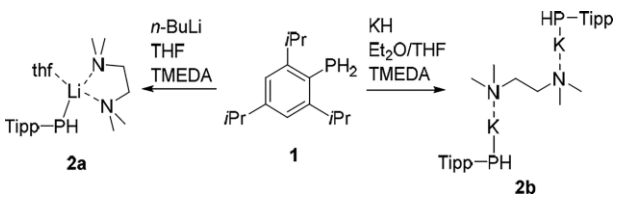

Scheme 3. Metalation of Tipp-PH_2 (**1**) and synthesis of lithium (**2a**) and potassium 2,4,6-triisopropylphenylphosphanide (**2b**).

The lithium derivative **2a**, dissolved in diethyl ether, was quickly added to a precooled solution (–50 °C) of bis(4-*tert*-butylphenyl)phosphinic chloride in diethyl ether (Scheme 4). After stirring for one hour at –40 °C the yellow solution was filtered through a frit that was covered with diatomaceous earth. From an aliquot of the filtrate all volatiles were removed under reduced pressure and the residue dried in vacuo. Thereafter this material was redissolved in [D_8]THF and investigated by ^{31}P NMR spectroscopy.

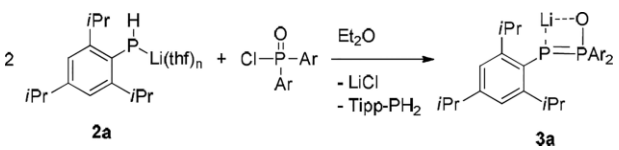

Scheme 4. Metathetical reaction of LiP(H)-C_6H_2–2,4,6-*i*Pr_3 with bis(4-*tert*-butylphenyl)phosphinic chloride.

This solution showed several phosphorus-containing compounds that could be identified unambiguously. The metathesis product **3a** with a P–P bond could be recognized by the large $^1J_{PP}$ coupling constant of approx. 511 Hz and two resonances at δ = +55.1 and –126.2 ppm. However, other compounds also formed during this reaction. Lithium diarylphosphinite (**4a**, δ = +88.1 ppm), excess LiP(H)-Tipp (δ = –161.6 ppm) and Tipp-PH_2 as well as the *meso* and *R*,*R*/*S*,*S* isomers of the diphosphane Tipp-P(H)-P(H)-Tipp (**5**, δ = –113.5 and –118.0 ppm) could be assigned without any doubt. In the proton-coupled ^{31}P NMR spectrum, the characteristic XX' part of an AA′XX′

spectrum could be assigned (see Supporting Information). In addition, a resonance at δ = +25.7 ppm with rather low intensity was observed which could hint toward the formation of $Ar_2P(O)–O–P(O)Ar_2$. This compound could arise from a well-known disproportionation of the lithium phosphinite Li–O–PAr_2 into the lithium phosphanide $LiPAr_2$ and the lithium phosphinate $LiO–P(O)Ar_2$ as described earlier,[20] followed by the reaction of the latter phosphinate complex with still present phosphinic chloride.

We also reacted KP(H)-Tipp with a stoichiometric amount of bis(4-*tert*-butylphenyl)phosphinic chloride and monitored the reaction again by ^{31}P NMR spectroscopy. As before we observed the targeted potassium complex $Ar_2P(O)$-P(K)Tipp (**3b**) that could be unambiguously assigned by characteristic chemical shifts (δ = +53.4 and –126.4 ppm) and the large $^1J_{PP}$ coupling constant of 481 Hz. However, this complex degraded fast to the potassium diarylphosphinite **4b** and to the *meso* and *R*,*R*/*S*,*S* isomers of the diphosphane Tipp-P(H)-P(H)-Tipp (**5**) as observed for the lithium derivative, too.

Based on these observations, we propose a mechanism for the degradation of $Ar_2P(O)$-P(M)-Tipp [M = Li (**3a**), K (**3b**)] that is depicted in Scheme 5. The P–P bond breaks rather easily, producing well-known metal diarylphosphinites M–O–PAr_2 and 2,4,6-triisopropylphenylphosphinidene. Due to the fact that phosphinidenes have an electron sextet they are extremely reactive. Thus these short-lived species attack Tipp-PH_2 and insert immediately into a P–H bond yielding 1,2-bis(2,4,6-triisopropylphenyl)diphosphane (**5**).

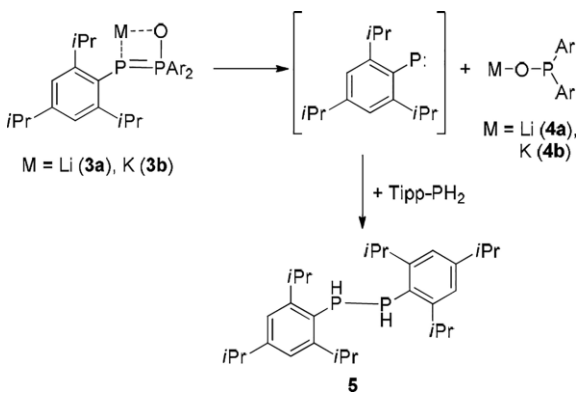

Scheme 5. Proposed mechanism for the degradation of **3a** and **3b** via cleavage of the P–P bond, formation of the intermediate phosphinidene which inserts into a P–H bond of Tipp-PH_2.

Molecular Structures

Lithium phosphanides represent a well-recognized substance class with many representatives.[21] The molecular structure and atom labeling scheme of mononuclear [(thf)(tmeda)Li-P(H)-Tipp] (**2a**) are depicted in Figure 1. The lithium atom has a distorted tetrahedral coordination sphere with a Li–P bond length of 264.4(9) pm. The structure is comparable to those of other lithiated primary phosphanes such as, for example, [$(thf)_3$Li-P(H)-Mes],[22] [(thf)(tmeda)Li-P(H)-Mes],[23] [$(py)_3$Li-P(H)-Mes*],[24] and [$(thf)_3$Li-P(H)-Mes*].[25] The P–C bond length of 184.1(4) pm is a typical single bond value without interaction of the aryl π-system and the P-centered electron pair. The pyramidal environment of the phosphorus atom [P1-bound $H1_{P1}$ atom was found and isotropically refined, angle sum of P1: 297(2)°] is in agreement with this interpretation. Intramolecular steric repulsion leads to significantly different P1–C1–C2/6 bond angles.

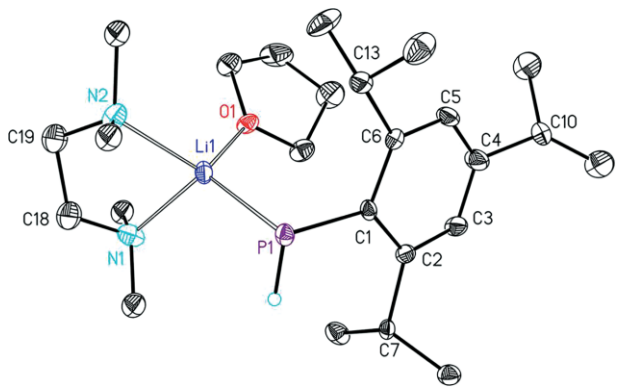

Figure 1. Molecular structure and atom labeling scheme of [(thf)(tmeda)Li-P(H)-Tipp] (**2a**). The ellipsoids represent a probability of 30 %. C-bound hydrogen atoms are omitted for clarity reasons. Selected bond lengths /pm: Li1–O1 195.5(9), Li1–N1 215.2(9), Li1–N2 211.8(10), Li1–P1 264.4(9), P1–$H1_{P1}$ 132(4), P1–C1 184.1(4); angles / °: Li1–P1–C1 95.4(2), Li1–P1–$H1_{P1}$ 101(2), C1–P1–$H1_{P1}$ 100.7(19), P1–C1–C2 125.6(4), P1–C1–C6 118.2(4), C2–C1–C6 116.2(4).

The molecular structure and atom labeling scheme of $[(tmeda)_{0.5}$K-P(H)-Tipp$]_\infty$ (**2b**) is shown in Figure 2. The po-

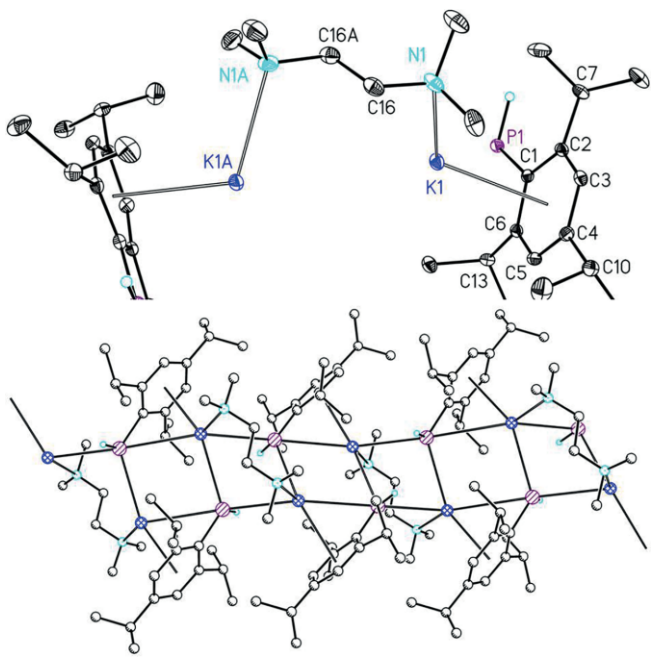

Figure 2. Molecular structure and atom numbering scheme of $[(tmeda)_{0.5}$K-P(H)-Tipp$]_\infty$ (**2b**, top). The ellipsoids represent a probability of 30 %, C-bound hydrogen atoms are neglected for the sake of clarity. Selected bond lengths /pm: K1–N1 297.3(2), K1–P1 377.13(9), K1–P1A 330.49(9), K1–P1B 330.82(8), K1–C1 300.9(2), K1–C2 322.3(2), K1–C3 347.4(2), K1–C5 340.6(2), P1–C1 182.7(2); angles / °: P1–C1–C2 125.95(19), P1–C1–C6 117.43(18), C2–C1–C6 116.6(2). At the bottom, a cut-out of the strand structure is depicted.

tassium atom K1 is side-on bound to one arylphosphanide ligand [K1–P1 377.13(9) pm] and two shorter contacts to neighboring phosphanides are observed [K1–P1A 330.49(9) and K1–P1B 330.82(8) pm]. This coordination behavior leads to formation of an undulated strand structure of alternating potassium and phosphorus atoms. The potassium atoms of every second four-membered K_2P_2 ring are bridged by a tmeda ligand with K1–N1 bond lengths of 297.3(2) pm. The P1–C1 bond length of 182.7(2) pm is slightly shorter than observed for the lithium congener **2a** supporting a weak interaction between the lone pair at P and the π-system of the aryl group.

The thf adduct $[(thf)_2K\text{-}P(H)\text{-}Tipp]_\infty$ forms a strand structure in the crystalline state, too, but here two one-dimensional K-P(H)-Tipp chains are interconnected by bridging thf bases.[26] However, the rubidium congener $[(thf)Rb\text{-}P(H)\text{-}Tipp]_\infty$ shows a comparable wavy ladder structure.[26] In contrast to this aggregation behavior, the smaller mesityl substituents lead to a three-dimensional polymeric structure[27] whereas three-dentate pmdeta bases are able to stabilize dinuclear structures of the type $[(pmdeta]K\text{-}P(H)\text{-}Mes]_2$.[28] Larger terphenyl groups lead to lower aggregation degrees[29] and the crown ether is even able to form mononuclear [(18-C-6) K-P(H)-Mes*].[30]

The molecular structure and atom labeling scheme of 1,2-bis(2,4,6-triisopropylphenyl)diphosphane (**5**) is depicted in Figure 3. The P-bound hydrogen atoms are disordered due to co-crystallization of *meso* and *R*,*R*/*S*,*S*-isomeric molecules. The P1–P1A [221.8(1) pm] and P1–C1 bond lengths [184.6(2) pm] lie in the expected ranges as also observed for 1,2–dimesityldiphosphane (P–P 222.84[11], P–C 183.7(2) pm) and 1,2-bis(2,6-diisopropylphenyl)diphosphane [P–P 220.60(8), P–C 184.14(13) pm].[31]

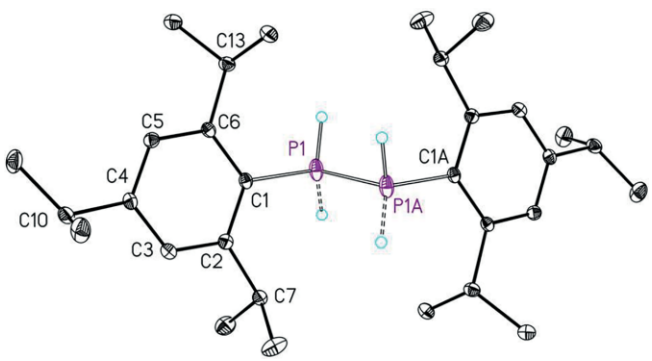

Figure 3. Molecular structure and atom labeling scheme of 1,2-bis(2,4,6-triisopropylphenyl)diphosphane (**5**). The ellipsoids represent a probability of 30 %, C-bound hydrogen atoms are omitted for the sake of clarity. Selected bond lengths /pm: P1–P1A 221.80(10), P1–C1 184.62(18); angles /°: P1–C1–C2 119.44(14), P1–C1–C6 121.07(13), C2–C1–C6 119.45(16).

Due to ongoing degradation processes during crystallization efforts, an isolation of analytically pure $Ar_2P(O)\text{-}P(Li)Tipp$ (**3a**) failed. Nevertheless, we could crystallize a complex of the type $[\mathbf{3a}\cdot\mathbf{4a}\cdot LiCl\cdot 2Et_2O]_2$ from diethyl ether. The molecular structure and atom labeling Scheme of this complex is depicted in Figure 4. The central four-membered $(LiCl)_2$ ring contains a crystallographic center of symmetry and Li-Cl distances of 241.2(5) and 245.2(5) pm. Such dimeric $[(L)_2LiCl]_2$ structures have been observed earlier in e.g. $[(thf)_2Li(\mu\text{-}Cl)]_2$ with slightly shorter Li–Cl bonds of 230.8(3) and 234.2(3) pm.[32] Lithium[33] and potassium diarylphosphinites form tetranuclear complexes with inner M_4O_4 heterocubane cores.[34] In these cage compounds the phosphinite oxygen atoms bridge three alkali metal atoms. In $[\mathbf{3a}\cdot\mathbf{4a}\cdot LiCl\cdot 2Et_2O]_2$ the diarylphosphinite substructures show comparable binding properties and O5 is positioned above the plane of Li1, Li2 and Li3 with Li-O5 bond lengths of 196.7(5), 200.6(5) and 189.7(5) pm, respec-

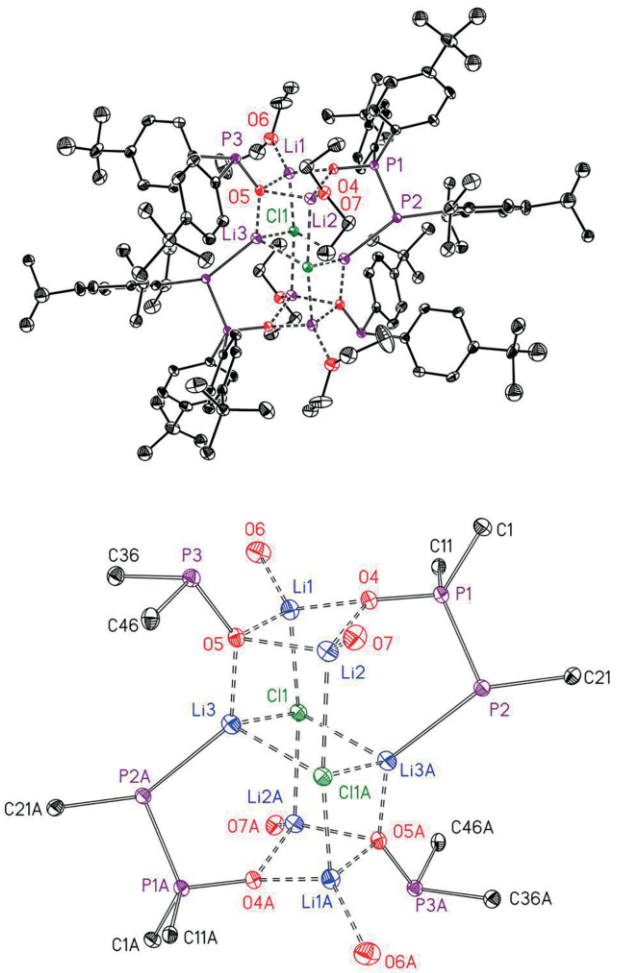

Figure 4. Molecular structure and atom labeling Scheme of $[\mathbf{3a}\cdot\mathbf{4a}\cdot LiCl\cdot 2Et_2O]_2$ (top) The ellipsoids represent a probability of 30 %, hydrogen atoms are omitted for clarity reasons. Selected bond lengths /pm: P1–P2 210.50(10), P1–C1 181.6(3), P1–C11 182.4(3), P1–O4 153.69(19), P2–C21 186.4(3), P2–Li3A 256.4(5), Li1–Cl1 246.6(5), Li1–O4 190.0(5), Li1–O5 196.7(5), Li1–O6 197.1(5), Li2–Cl1A 247.9(5), Li2–O4 193.2(5), Li2–O5 200.6(5), Li2–O7 196.3(5), Li3–Cl1 241.2(5), Li3–Cl1A 245.2(5), Li3–O5 189.7(5); angles /°: P1–P2–C21 105.51(9), P1–P2–Li3A 102.86(12), C21–P2–Li3A 144.58(14), P2–P1–O4 106.17(8), P2–P1–C1 114.80(9), P2–P1–C11 115.57(9), O4–P1–C1 108.63(12), O4–P1–C11 106.32(11), C1–P1–C11 104.93(12), P2–C21–C22 118.3(2), P2–C21–C26 123.1(2), C22–C21–C26 118.4(3). At the bottom, the inner cage is depicted to clarify the bonding situation. Hydrogen and carbon atoms are omitted with the exception of the *ipso*-carbon atoms.

tively. The P3–O5 bond length of 160.12(19) pm is slightly elongated compared to the distances in tetranuclear lithium diphenylphosphinite [P–O between 158.4(2) and 158.8(2) pm].[33] All lithium atoms have distorted tetrahedral coordination spheres, Li1 and Li2 complete their coordination number by ligated diethyl ether ligands [Li1–O6 197.1(5), Li2–O7 196.3(5) pm]. The Li1–O4 and Li2–O4 bonds are the shortest Li–O distances due to the smaller coordination number of 3 for O4. In addition, the enhanced electrostatic attraction between the negatively charged oxygen atom and the lithium cation also shortens these Li-O4 contacts.

The phosphanidylphosphane oxide Tipp-P–P(O)Ar_2 substructure has a P1–P2 bond length of 210.50(10) pm. The O4 atom is bound at P1 [153.69(19) pm] and bridges the lithium atoms Li1 and Li2. The P2 atom coordinates to Li3A with a distance of 256.4(5) pm which is smaller than observed in mononuclear **2a** and supports significant electrostatic attraction between the lithium cation and the P2 atom. The P2–C21 bond length is slightly larger than observed in the alkali metal phosphanides **2a** and **2b**. We interpret these findings in the sense of a phosphanidyl-phosphonium oxide as depicted in Scheme 6.

Scheme 6. Schematic representation of the mesomeric forms of the substructure of the anion of **3a** with ionic and covalent P–P bonding modes (see text, Ar = C_6H_4-4-*t*Bu).

In order to correlate P–P bond order, oxidation state and coordination number of the phosphorus atoms and P–P bond lengths, diverse P-containing compounds are compared in Table 1. The P–O bond lengths lie in a very narrow range (entries 3–7 and 12–14) with the exception of the lithium diarylphosphinites (entries 10 and 11) with large values due to the coordination number of four for the oxygen atoms (μ_3-coordination mode of the phosphinite ligands). The P–P bond lengths depend on the coordination number of P with the shortest P–P bonds of approx. 203–205 pm in diphosphenes (entry 1) symptomatic for P=P double bonds. Diphosphanes have a typical single bond of approx. 222 pm (entry 2). Mono-oxidation leads to a slight shortening (entries 5 and 6), whereas the doubly oxidized diphosphane dioxide has a longer P–P bond due to electrostatic repulsion between the positively charged P atoms. (entry 7). Charge delocalization shortens the P–P bonds (entries 8 and 9). Deprotonation of a diphosphane monoxide leads to rather short P–P bonds with partly double bond character, supported by electrostatic attraction between a negatively charged phosphanide unit and a phosphoryl moiety with a positively polarized P atom (entries 14 and 15). The P1–O4 bond length (entry 15) is significantly larger than observed for phosphane oxides with mainly P–O double bond character (entries 3–7) but this bond is also elongated compared to the P–O bond in lithium diarylphosphinate (formal bond order of 1.5, entry 12) supporting a dominating single bond character of the P1–O4 bond. The bridging coordination mode of the P1–O4 unit and accompanying enhancement of the coordination number of O4 also make a contribution to the elongation of the P1–O4 bond.

The diverse products of the reaction of Tipp-P(H)Li or Tipp-P(H)K with bis(4-*tert*-butylphenyl)phosphinic chloride in diethyl ether at –50 °C can be explained by the following reaction sequence. Initially the metathesis product, Tipp-P(H)-P(O)Ar_2, is formed which is immediately lithiated by still present Tipp-P(H)Li yielding observable phosphanidylphosphane oxide, Tipp-P(Li)-P(O)Ar_2 [or Tipp-P=P(OLi)Ar_2 via 1,3-Li shift], besides Tipp-PH_2. The product Tipp-P(Li)-P(O)Ar_2 slowly degrades with formation of lithium diarylphosphinite, Li–O–PAr_2, and liberation of (unobserved) phosphinidene Tipp-P:. The phosphinidene inserts immediately into a P–H bond of Tipp-PH_2 leading to the formation of the observed diphosphane Tipp-P(H)-P(H)-Tipp. Lithium diarylphosphinite slowly dismutates into lithium diarylphosphanide $LiPAr_2$ and lithium diarylphosphinate LiO_2PAr_2. The latter compound can react with still present diarylphosphinic chlor-

Table 1. Comparison of selected P-containing compounds to elucidate the dependency between bond order and bond length for P–P and P–O bonds (average values are given without estimated standard deviations).

	Compound	P–P	P–O	Ref.
1	Ar-P=P-Ar	203–205	–	[35]
2	Tipp-P(H)-P(H)-Tipp (**5**)	221.8(1)	–	This work
3	$Ph_2P(O)H$	–	148.81(11)	[36]
4	$Mes_2P(O)H$	–	148.54(13)	[37]
5	Ar*P(H)-P(O)(H)Ar*	219.46(8)	147.8(2)	[7]
6	Mes*P(H)-P(O)$(OEt)_2$	218.54(7)	147.16(13)	[38]
7	Ph(*t*Bu)P(O)-P(O)(*t*Bu)Ph	227.4(1)	149.2	[39]
8	$[Ph_3P\text{-}PPh_3]^+$ $[AlCl_4]^-$	213.3(6)	–	[13]
9	[ArP(Ph)-P[Li$(thf)_3$]-P(Ph)Ar]	216.1	–	[13]
10	Ar_2POLi (**4a**) [a]	–	160.12(19)	This work
11	$[Ph_2POLi(thf)]_4$	–	158.6	[33]
12	$[Mes_2P(O)\text{-}OLi(thf)_2]_2$	–	149.9	[20]
13	$[Ph_2P(O)\text{-}N(Mes)Li(thf)_2]$	–	149.7	[11]
14	$[Ar^*P\text{-}P(O)(H)Ar^*]^-$ $[Im]^+$ [b]	210.99(11)	149.2(2)	[7]
15	Tipp-P(Li)-P(O)Ar_2 (**3a**) [a]	210.50(10)	153.69(19)	This work

a) Substructures of [**3a**·**4a**·LiCl·$2Et_2O]_2$. b) Im = 1,3,4,5-tetramethylimidazolium, bound via a C–H···O hydrogen bridge.

ide, yielding the observed diarylphosphinic anhydride $Ar_2P(O)–O–P(O)Ar_2$ [$\delta(^{31}P)$ = 25.7 ppm].[40] This proposed mechanism requires the assumption that the metathetical reaction step is significantly slower than the metalation and phosphinidene insertion steps.

Zurmühlen and *Regitz* performed the reaction of $LiP(SiMe_3)Mes$ with bis(*tert*-butyl)phosphinic chloride and observed the formation of Mes-P=P(OSiMe$_3$)*t*Bu$_2$ (δ_P = +96 and –213 ppm, $^1J_{PP}$ = 429 Hz) after immediate 1,3-shift of the trimethylsilyl group from the phosphorus to the oxygen atom.[41] In a preliminary study we tried to stabilize the phosphanidylphosphane oxide by a metathesis reaction of bulky $LiP(Si\mathit{i}Pr_3)Mes$ (**6a**) with bis(4-*tert*-butylphenyl)phosphinic chloride in THF. For this experiment we have chosen the triisopropylsilyl group to shield the reactive P–P bond and to decelerate degradation. Again the ^{31}P NMR spectra unambiguously verified a fast 1,3-silyl shift from P to O and the quantitative formation of the targeted product Mes-P=P(OSi*i*Pr$_3$)Ar$_2$ (**8a**) (δ_P = 76.4 and –118.2 ppm, $^1J_{PP}$ = 623 Hz). However, within very few hours a complete degradation occurred and could quantitatively be monitored by addition of triphenylphosphane as an internal standard. The time-dependent first-order decomposition is depicted in Figure 5.

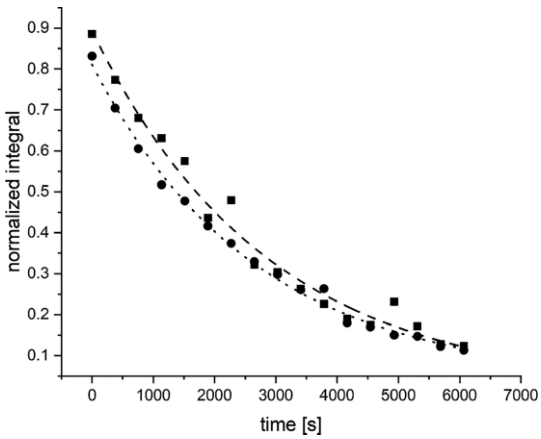

Figure 5. Degradation of Mes-P=P(OSi*i*Pr$_3$)(C$_6$H$_4$-4-*t*Bu)$_2$ (**8a**) in THF at room temperature, monitored for the resonances at δ = –118.2 (black circles) and 76.4 ppm (black squares) via ^{31}P NMR spectroscopy with the internal PPh_3 standard. The exponentially fitted curves are drawn with broken lines.

To study the influence of the bulkiness of the aryl group we prepared Tipp-P=P(OSi*i*Pr$_3$)Ph$_2$ (**8b**) analogously and monitored its decay by ^{31}P NMR spectroscopy. The substitution of the Mes group by the bulkier Tipp substituent decelerated the degradation process significantly by the factor of 3, yielding Ph_2P-OSi*i*Pr$_3$ (**9b**) as the major degradation end product. Thus, after approx. 1.5 hours at room temperature only half of the amount of Tipp-P=P(OSi*i*Pr$_3$)Ph$_2$ (**8b**) was still present in THF solution.

Presumably, the degradation proceeded analogously to the above discussed pathway. The half-life time was significantly larger because the bulky triisopropylsilyl substituent shielded the reactive P=P bond much more effectively than the alkali metal ions. Generally, Si–O bonds are very strong whereas M–O bonds are quite labile, often enabling the formation of solvent-separated ion pairs in ethereal solutions. After the 1,3-triisopropylsilyl shift the P=P bond was cleaved yielding the established trialkylsilylphosphinite (**9a**), which was identified by ^{31}P NMR spectroscopy (δ_P = 98.3 ppm), as the major end product as depicted in Scheme 7. The intermediately formed phosphinidene was very reactive and immediately trapped forming secondary yet unknown degradation products.

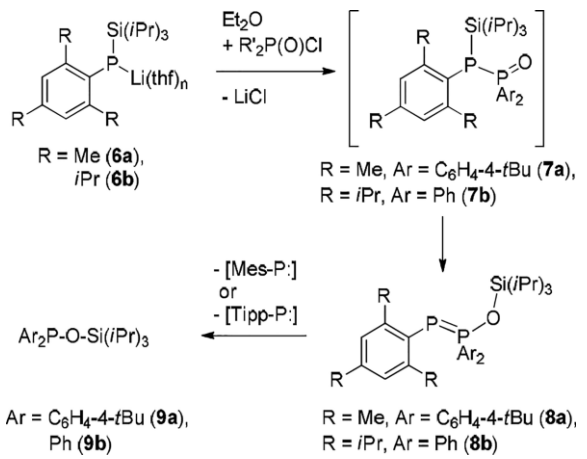

Scheme 7. Metathetical reaction of LiP(Si*i*Pr3)-C$_6$H$_2$-2,4,6-R [R = Me (**6a**), *i*Pr (**6b**)] with bis(aryl)phosphinic chloride yielding complexes **8a** and **8b**, respectively, which degrade to the triisopropylsiloxy-bis(aryl) phosphanes (**9a**: Ar = 4-*tert*-butylphenyl and **9b**: Ar = Ph) as the major secondary degradation product.

Enhancement of steric shielding by substitution of the mesityl group by a Tipp substituent decelerated the degradation, but again the trialkylsilyl-diarylphosphinite (trialkylsiloxy-diarylphosphane) was identified and the enormous reactivity of the liberated triisopropylphenyl-phosphinidene led to secondary products.

NMR Spectroscopy

The phosphanidylphosphane oxides show characteristic ^{31}P NMR spectra which are summarized in Table 2. The protonated derivatives have $^1J_{PP}$ coupling constants that are indicative of a P-P single bond and the hydrogen atom is bound at the phosphanyl unit giving R-P(H)-P(O)R′$_2$ (entries 1 and 2). In the imidazolium salt a hydrogen bridge is formed between the imidazolium cation and the phosphoryl moiety (entry 3). Furthermore, the alkali metal congeners (entries 9–16) form contact ion pairs with rather large $^1J_{PP}$ coupling constants. These values are in the same order of magnitude as observed for the silylated congeners (entries 4–8), which contain strong Si–O bonds, supporting a P–P multiple bond in all these derivatives. In contrast, the $^1J_{PP}$ values of the hydrogen-substituted congeners with P-bound hydrogen atoms (entries 1 and 2) are roughly only half as large.

A comparison of the Mes and Tipp substituted phosphanidylphosphane oxides with M = Si*i*Pr$_3$ (entries 6 and 8), Li (entries 11 and 12), and potassium (entries 15 and 16) shows a decreasing $^1J_{PP}$ coupling constant supporting decreasing P–P

Table 2. Selected NMR parameters for compounds of the general type RP=P(OM)R′$_2$ regardless of the essentially contributing mesomeric form (see Scheme 6).

	R [a]	R′ [a]	M	δ_P(RP)	δ_P(PO)	$^1J_{PP}$	Ref.
1	Mes*	OEt	H	–88.8	+35.0	222	[38]
2	Ter	H/Ter	H	–77.4	+9.6	248.7	[7]
3	Ter	H/Ter	Im [b]	–46.8	+28.5	464.2	[7]
4	Mes	*t*Bu	$SiMe_3$	–213	+96	429	[41]
5	Mes	Alkyl [c]	$SiMe_3$	–209	+78	433	[41]
6	Tipp	Ph	$Si*i*Pr_3$	–143.2	+81.2	634	[42]
7	Tipp	Ph	$SiMe_3$	–132.5	+77.8	628	[42]
8	Mes	Ar	$Si*i*Pr_3$	–118.2	+76.4	623	This work
9	Mes*	OEt	Li	n.a. [d]	n.a. [d]	615	[38]
10	CN	NMe_2	Li	–205.0	+73.6	347.9	[13]
11	Mes	Ar	Li	–103.7	+53.2	501	[42]
12	Tipp	Ar	Li	–126.2	+55.1	511.5	This work
13	CN	Ph	Na	–161.4	+55.7	362.5	[13]
14	CN	OEt	Na	–202.8	+68.5	392.5	[13]
15	Mes	Ar	K	–103.9	+53.5	484	[42]
16	Tipp	Ar	K	–126.4	+53.4	481	This work

a) Ar = 4-*tert*-butylphenyl, Mes = 2,4,6-trimethylphenyl, Mes* = 2,4,6-tri(*tert*-butyl)phenyl, Ter = 2,6-dimesitylphenyl, Tipp = 2,4,6-triisopropylphenyl. b) Im = 1,3,4,5-tetramethylimidazolium. c) Alkyl = 2,3,4-trimethylpentane-2,4-diyl. d) n.a. = not assigned.

double bond character caused by an increasing electrostatic attraction between M and the phosphanidylphosphane oxide anion (see Scheme 6). This interpretation is in agreement with the observation that phosphanylphosphane oxides (entries 1 and 2) exhibit the smallest coupling constants between the P atoms, indicative for a P–P single bond. It is noteworthy that for RP=P(OSiR"$_3$)R′$_2$ with R′ = alkyl (entries 4 and 5) the $^1J_{PP}$ coupling constants are apparently significantly smaller than for derivatives with R′ = aryl (entries 6–8).

Conclusions

The reaction of lithium (**2a**) and potassium 2,4,6-triisopropylphenylphosphanide (**2b**), MP(H)-Tipp, with bis(4-*tert*-butylphenyl)phosphinic chloride, $Ar_2P(O)Cl$, yields the unobserved metathesis product, Tipp-P(H)-P(O)Ar_2. This intermediate immediately reacts with another equivalent of MP(H)-Tipp, leading to the formation of Tipp-P=P(OM)Ar_2 [M = Li (**3a**) and K (**3b**)] and Tipp-PH_2 (**1**). The phosphanidylphosphane oxides **3a** and **3b** slowly degrade under release of the extremely reactive phosphinidene Tipp-P: with an electron sextet. This unobserved species inserts immediately into a P–H bond of Tipp-PH_2 yielding the diphosphane Tipp-P(H)-P(H)-Tipp (**5**). The compounds have unambiguously been identified by their characteristic ^{31}P NMR spectra with typical chemical shifts and coupling constants. Furthermore, the major products have been verified by crystal structure determinations of **2a**, **2b**, **5**, and the unique co-crystallization product [**3a**·**4a**·LiCl·2Et_2O]$_2$. The latter molecular structure allows for the first time to elucidate the P–P bond length in a mixed-valent phosphorus derivative of the type Ar-P=P(OM)Ar_2. The proposed reaction sequence is depicted in Scheme 8. Unobserved intermediates are included in square brackets.

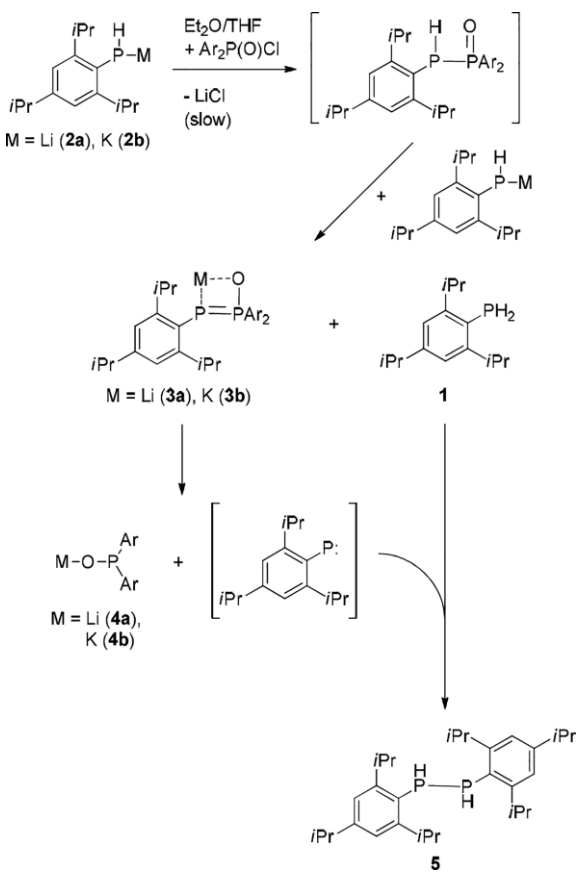

Scheme 8. Sequence of the reaction of MP(H)-Tipp with diarylphosphinic chloride with a 2:1 stoichiometry. Compounds in square brackets are unobserved whereas all other compounds have been identified unambiguously by ^{31}P NMR spectroscopy and/or X-ray structure analysis.

In addition to these experiments we tried to stabilize the P–P multiple bond by trialkylsilyl substituents. Thus the metathesis

reaction of $LiP(SiR_3)Ar^*$ (Ar* = Mes, Tipp; R = Me, *i*Pr) with diarylphosphinic chloride, $Ar_2P(O)Cl$, yields quantitatively $Ar^*\text{-}P{=}P(OSiR_3)Ar_2$. This metathesis product releases the unobservable phosphinidene Ar*–P:, which immediately forms secondary degradation products, and the already known trialkylsiloxy-diarylphosphanes (trialkylsilyl-diarylphosphinites) are formed.

The compounds with the P–P multiple bonds, the alkali metal phosphanidyl-diarylphosphane oxides **3a** and **3b** as well as the silylated congeners $Ar^*\text{-}P{=}P(OSiR_3)Ar_2$ **8a** and **8b**, exhibit characteristic chemical $\delta(^{31}P)$ shifts for the two- and four-coordinate P atoms and large $^1J_{PP}$ coupling constants. These coupling constants increase in the series **3b**, **3a** and $Ar^*\text{-}P{=}P(OSiR_3)Ar_2$ in agreement with the expectation that a strengthening of the O–M bond from the ionic O–K interaction to O–Li and finally to very strong O–Si bonds and hence decreasing ionic character lead to increasing P–P double bond character and to larger coupling constants. These silyl derivatives $Ar^*\text{-}P{=}P(OSiR_3)Ar_2$ also release the phosphinidene Ar*-P: yielding trialkylsilyl-diarylphosphinites and secondary by-products. Bulky groups Ar* and SiR_3 decelerate degradation processes.

In conclusion, derivatives of the type $Ar^*\text{-}P{=}P(OM)Ar_2$ (M = Li, K) and $Ar^*\text{-}P{=}P(OSiR_3)Ar_2$ (Ar = aryl, Ar* = bulky aryl, R = alkyl) are intrinsically unstable and release highly reactive phosphinidene species Ar*-P: (which form secondary degradation products), leaving the well-known phosphinites of the type $Ar_2P\text{–}OM$ and $Ar_2P\text{–}O\text{–}SiR_3$, respectively.

Experimental Section

General Remarks: All manipulations were carried out under an inert nitrogen atmosphere using standard Schlenk techniques. The solvents were dried with KOH and subsequently distilled over sodium/benzophenone in a nitrogen atmosphere prior to use. Deuterated solvents were dried with sodium, distilled, degassed, and stored in nitrogen over sodium. ^1H, $^{13}C\{^1H\}$ and $^{31}P\{^1H\}$ NMR spectra were recorded on Bruker Avance III 400. Chemical shifts are reported in parts per million relative to $SiMe_4$ (^1H, ^{13}C) as an external standard referenced to the solvents residual signals.[43] IR spectra were recorded on a Bruker Alpha spectrometer. Due to the extreme sensitivity of the phosphanides of lithium (**2a**) and potassium (**2b**) toward air, these compounds were covered with nujol prior to the IR measurement. All substrates were purchased from Alfa Aesar, abcr, Sigma Aldrich or TCI and used without further purification. 2,4,6-Triisopropylphenylphosphane (**1**)[44] and its lithium[45] and potassium salts have been prepared via modified procedures described earlier.[26] The yields given are not optimized. Purity of the compounds was verified by NMR spectroscopy. The objective of this study was the elucidation of structural parameters for an alkali metal phosphanidylphosphane oxide and mechanistic studies of its decay in ethereal solvents, based on NMR experiments.

Caution: Isolated and dried lithium and potassium phosphanides **2a** and **2b** inflame spontaneously if exposed to air. Therefore, we did not accomplish combustion analyses of these compounds.

Synthesis of 2,4,6-Triisopropylphenylphosphane (1): A three neck round-bottomed flask with reflux condenser and dropping funnel was loaded with 3.4 g of Mg (132 mmol) and 100 mL of THF. Bromo-2,4,6-triisopropylbenzene (17 g, 60 mmol) was added dropwise until the Grignard reaction started. The remaining bromo-2,4,6-triisopropylbenzene was added slowly to keep the solution under reflux conditions. After complete addition of the bromoarene the mixture was heated to reflux for additional 1.5 h. After cooling to room temperature, the Grignard reagent was added dropwise under vigorous stirring at –78 °C to 15 mL of PCl_3 (171 mmol) in a two neck round-bottomed flask. During addition the solution turned yellow and a white solid precipitated. The mixture was heated to room temperature and was stirred for additional 0.5 h. All volatiles were removed under reduced pressure. The remaining solid was suspended in 100 mL of Et_2O and filtered. The filtration residue was washed two times with 20 mL of Et_2O. The volume of the combined ethereal filtrates was reduced to 40 mL. DIBAL-H/*n*-hexane (150 mL of a 1 M solution, 150 mmol) was added dropwise at –50 °C. The orange solution was heated to room temperature and stirred for 1 h. Conversion to the phosphane was monitored by ^{31}P NMR spectroscopy. Excess of DIBAL-H was carefully quenched with 40 mL of degassed water at 4 °C. After separation of the organic layer the aqueous phase was extracted twice with 20 mL of *n*-pentane. The solvent of the organic extracts was evaporated. Subsequently, 2,4,6-triisopropylphenylphosphane (**1**) was isolated as a colorless liquid by vacuum distillation (6×10^{-2} mbar, 85–95 °C). Yield: 9.54 g (40.4 mmol), 68 %. **^1H NMR** (400.13 MHz, C_6D_6, 297 K): δ = 7.08 (d, $^4J_{P,H}$ = 2.4 Hz, 2 H, *meta-H*), 3.84 (d, $^1J_{P,H}$ = 203.2 Hz, 2 H, *-PH*$_2$), 3.45 [heptd, $^4J_{P,H}$ = 3.2, ^3J(H,H) = 6.7 Hz, 2 H, *ortho-CH(iPr)*], 2.77 [hept, $^3J_{H,H}$ = 6.9 Hz, 1 H, *para-CH(iPr)*], 1.22 [d, $^3J_{H,H}$ = 7.0 Hz, 6 H, *para-CH*$_3$*(iPr)*], 1.21 [d, $^3J_{H,H}$ = 6.9 Hz, 12 H, *ortho-CH*$_3$*(iPr)*]. **$^{13}C\{^1H\}$ NMR** (100.62 MHz, C_6D_6, 297 K): δ = 152.3 (d, *J* = 9.7 Hz, *ortho-C*), 149.2 (s, *para-C*), 122.9 (d, *J* = 12.9 Hz, *ipso-C*), 121.3 (d, *J* = 2.8 Hz, *meta-C*), 34.8 [s, *para-CH(iPr)*], 33.3 [d, *J* = 11.6 Hz, *ortho-CH(iPr)*], 24.3 [s, *para-CH*$_3$*(iPr)*], 23.9 [s, *ortho-CH*$_3$*(iPr)*]. **^{31}P NMR** (161.98 MHz, C_6D_6, 297 K): δ = –159.0 (tm, $^1J_{P,H}$ = 203.2 Hz). **IR** (nujol): $\tilde{\nu}$ = 2959 (s), 2924 (s), 2864 (s), 2297 (m), 1600 (w), 1559 (w), 1527 (w), 1459 (s), 1417 (s), 1380 (m), 1359 (m), 1313 (m), 1300 (m), 1256 (m), 1237 (w), 1189 (m), 1166 (w), 1127 (m), 1105 (m), 1060 (s), 1041 (m), 941 (w), 922 (w), 884 (s), 871 (s), 829 (w), 807 (w), 754 (s), 732 (m), 714 (m), 640 (m), 623 (m), 510 (m) cm^{-1}.

Synthesis of (tmeda)(thf)lithium 2,4,6-Triisopropylphenylphosphanide (2a): $TippPH_2$ (**1**, 1 g, 4,23 mmol) was dissolved in 20 mL of *n*-hexane. Then 2,6 mL of 1.6 M BuLi/*n*-hexane (4.23 mmol) were added dropwise at –78 °C. The solution was slowly heated to room temperature and stirred for 2 h. Evaporation to dryness under reduced pressure yielded an amorphous yellow powder. Crystallization could be achieved from a solvent mixture of THF/*n*-hexane/TMEDA at –20 °C. Yield: 1 g (4.13 mmol), 98 %. **^1H NMR** (400.13 MHz, [D_8]THF, 297 K): δ = 6.60 (s, 2 H, *meta-H*), 3.74 [s, 2 H, *ortho-CH(iPr)*], 2.69 [s, 1 H, *para-CH(iPr)*], 2.06 (d, $^1J_{P,H}$ = 164.5 Hz, 2 H,, *-PH*$_2$), 1.21 [d, *J* = 6.8 Hz, 12 H, *ortho-CH*$_3$*(iPr)*], 1.18 [d, *J* = 6.9 Hz, 6 H, *para-CH*$_3$*(iPr)*]. **$^{13}C\{^1H\}$ NMR** (100.62 MHz, [D_8]THF, 297 K): δ = 152.7 (*ipso-C*), 146.6 (*ortho-C*), 137.2 (*para-C*), 118.8 (*meta-C*), 35.3 [*para-CH(iPr)*], 33.3 [d, *J* = 14.8 Hz, *ortho-CH(iPr)*], 25.2 [*para-CH*$_3$*(iPr)*], 24.2 [*ortho-CH*$_3$*(iPr)*]. **^{31}P NMR** (161.98 MHz, [D_8]THF, 297 K): δ = –166.4 (d, $^1J_{P,H}$ = 165.4 Hz).

Synthesis of Semi(tmeda)potassium 2,4,6-Triisopropylphenylphosphanide (2b): To a suspension of 200 mg of KH (4.99 mmol) in a mixture of 7 mL of Et_2O and 2 mL of THF, 876 mg of (2,4,6-triisopropylphenyl)phosphane were added at 0 °C. After removal of the cooling bath, evolution of hydrogen gas was observed. After stirring for 12 h the excess of KH was removed by filtration. The yellow filtrate was evaporated to dryness under reduced pressure yielding an amorphous yellow solid. Crystallization could be achieved from a sol-

vent mixture of Et_2O/TMEDA with a ratio of 20:1. Yield (amorphous solid): 982 mg. ^{31}P-NMR titration (internal standard: Ph_3P) verified a quantitative conversion. **IR** (nujol): $\tilde{\nu}$ = 3502 (w), 2953 (s), 2926 (s), 2888 (s), 2864 (s), 2259 (m), 1987 (w), 1766 (w), 1665 (w), 1593 (m), 1535 (w), 1460 (s), 1411 (s), 1377 (m), 1360 (m), 1306 (m), 1252 (m), 1237 (m), 1252 (m), 1237 (m), 1224 (m), 1165 (m), 1127 (m), 1100 (m), 1057 (s), 1038 (s), 939 (m), 920 (m), 878 (s), 808 (w), 755 (m), 731 (w), 714 (w), 636 (m), 622 (m), 562 (w), 514 (w), 479 (w), 425(w). **^{1}H NMR** (400.13 MHz, [D_8]THF, 297 K): δ = 6.57 (s, 2 H, *meta-H*), 3.67 [m, $^4J_{P,H}$ = 6.4 Hz, 2 H, *ortho-CH(iPr)*], 2.65 [hept, $^3J_{H,H}$ = 6.9 Hz, 1 H, *para-CH(iPr)*], 1.18 [d, $^3J_{H,H}$ = 6.8 Hz, 12 H, *ortho-CH_3(iPr)*], 1.14 [d, $^3J_{H,H}$ = 7.0 Hz, 6 H, *para-CH_3(iPr)*]. **^{13}C{^{1}H} NMR** (150.93 MHz, [D_8]THF, 297 K): δ = 154.7 (*ipso-C*), 145.77 (*ortho-C*), 135.7 (*para-C*), 118.9 (*meta-C*), 35.3 [*para-CH(iPr)*], 33.1 [d, *J* = 15.0 Hz, *ortho-CH(iPr)*], 25.1 [*para-CH_3(iPr)*], 24.0 [*ortho-CH_3(iPr)*]. **^{31}P NMR** (161.98 MHz, [D_8]THF, 297 K): δ = –153.8 (d, $^1J_{P,H}$ = 153.1 Hz).

Synthesis of Lithium Phosphanidylphosphane Oxide (3a): Bis(4-*tert*-butylphenyl)phosphinic chloride (323 mg, 0,93 mmol) was suspended in 8 mL of Et_2O and cooled to –50 °C. TippPHLi (**2a**, 444 mg, 1,83 mmol) was dissolved in 12 mL of Et_2O and added quickly. After stirring for 1h at –40 °C the cloudy yellow solution was filtered through a frit covered with diatomaceous earth. An aliquot of the solution was evaporated to dryness and redissolved for NMR analysis in [D_8]THF. After 1 week at –20 °C crystals precipitated from an Et_2O solution. Crystallization of TippP(H)-P(H)Tipp was achieved after a month from DME solution. The NMR spectroscopic monitoring of this reaction gave the following NMR spectra: **^{31}P NMR** (162 MHz, [D_8]THF, 297 K): δ = 87.9 (s, *Ar_2POLi, **4a***), 55.1 (d, $^1J_{P,P}$ = 511.5 Hz, *P-P, **3a***), –113.47 [AA'XX', $^1J_{P,H}$ = 206.5, $^1J_{P,P}$ = 202, $^2J_{P,H}$ = 12.5, $^3J_{H,H}$ = 6 Hz, *D,L-(tippPH)*$_2$, ***5***], –118.02 [AA'XX', $^1J_{P,H}$ = 206.5, $^1J_{P,P}$ = 202, $^2J_{P,H}$ = 12.5, $^3J_{H,H}$ = 6 Hz, *meso-(tippPH)*$_2$, ***5***], –126.20 (d, *J* = 511.5 Hz, ***3a***), –161.57 (tm, $^1J_{P,H}$ = 203.4 Hz, *tippPHLi, **2a***). **^{31}P{^{1}H} NMR** (162 MHz, [D_8]THF, 297 K): δ = 88.1 (s, *Ar_2POLi*), 55.1 (d, $^1J_{P,P}$ = 511.5 Hz; *P-P*), 25.7 [s, *Ar_2P(O)-O-P(O)Ar_2*], –113.5 [s, *(tippPH)*$_2$], –118.02 [s, *(tippPH)*$_2$], –126.2 (d, $^1J_{P,P}$ = 511.5 Hz), –161.6 (s, *tippPHLi*). Due to the fact that pure **3a** was not accessible and that degradation of the cocrystallization product [**3a·4a·**LiCl·2Et_2O]$_2$ continued after dissolution in ethereal solvents, isolation of analytically pure **3a** and its further characterization did not succeed.

Synthesis of Mes-P=P(OSi*i*Pr$_3$)(C$_6$H$_4$-4-*t*Bu)$_2$ (8a): Potassium (2,4,6-triimethylphenyl)phosphanide (**2b**, 755 mg, 3.97 mmol) was dissolved in 16 mL of THF and dropwise added to a solution of triisopropylsilyl chloride (TIPS-Cl) in 10 mL of THF at –50 °C. Subsequently, 2.5 mL of 1.6 M/*n*BuLi in *n*-hexane were added at –78 °C. The resulting yellow solution was added to bis(4-*tert*-butylphenyl) phosphinic chloride (1.34 g, 3.84 mmol) in 40 mL of THF at –78 °C. A 0.4 mL aliquot was taken from solution, mixed with 0.1 mL of C_6D_6 and 15 mg of triphenylphosphane as internal standard and this solution was used for immediate NMR analysis of the quantitative degradation studies. **^{31}P NMR** (162 MHz, C_6D_6, 297K): δ = 98.3 (quin, J_{PH} = 7.6 Hz, **9a**), 76.4 (d, J_{PP} = 622.3 Hz, **8a**), 31.3 (s), 20.2 (s), –5.5 (sept, J_{PH} = 7.7 Hz, PPh_3), –110.2 (d, J_{PP} = 184.5 Hz;), –118.17 (d, *J* = 622.3 Hz, **8a**), –144.9 (t, J_{PP} = 184.5 Hz), –176.9 (d, J_{PH} = 214.5 Hz, MesP(H)TIPS).

Synthesis of Tipp-P=P(OSi*i*Pr$_3$)Ph$_2$ (8b): 2,4,6-Triisopropylphenylphosphane (**1**, 324 mg, 1.37 mmol) was dissolved in 5 mL of THF and cooled to –78 °C. Reagents were added in the following order: 1.6 M *n*BuLi/*n*-hexane (0.86 mL, 1.37 mmol), triisopropylsilyl chloride (TIPS-Cl, 0.29 mL, 1.37 mmol), 1.6 M *n*BuLi/*n*-hexane (0.86 mL, 1.37 mmol). The resulting yellow solution was added to bis(phenyl) phosphinic chloride (324 mg, 1.37 mmol) in 5 mL of THF at –78 °C. A 0.4 mL aliquot was taken from solution, mixed with 0.1 mL of C_6D_6 and 14 mg of triphenylphosphane and used for immediate NMR analysis of the degradation process. **^{31}P NMR** (162 MHz, C_6D_6, 297K): δ = 97.7 (quin, J_{PH} = 7.9 Hz, **9b**), 77.5 (dt, J_{PP} = 636.6, J_{PH} = 12.7 Hz, **8b**), 33.4 (s), 29.8 (s), 20.1 (s), –5.5 (sept, J_{PH} = 8.2 Hz, PPh_3), –100.23 (d, J_{PP} = 179.2 Hz), –133.5 (t, J_{PP} = 179.2 Hz), –147.0 (d, J_{PP} = 637.0 Hz, **8b**), –184.3 [d, J_{PH} = 212.2 Hz, TippP(H)TIPS].

X-ray Structure Determinations: The intensity data for the compounds were collected on a Nonius KappaCCD diffractometer using graphite-monochromated Mo-K_α radiation. Data were corrected for Lorentz and polarization effects; absorption was taken into account on a semi-empirical basis using multiple-scans.[46–48] The structures were solved by Direct Methods (SHELXS)[49] and refined by full-matrix least-squares techniques against F_o^2 (SHELXL-97[44] and SHELXL-2014[50]). All hydrogen atoms of **5** and those bonded to the phosphorus atoms P1 of compounds **2a** and **2b** were located by difference Fourier synthesis and refined isotropically. All other hydrogen atoms were included at calculated positions with fixed thermal parameters. All non-hydrogen atoms were refined anisotropically.[49,50] Crystallographic data as well as structure solution and refinement details are summarized in Table S1. XP[51] was used for structure representations.

Crystallographic data (excluding structure factors) for the structures in this paper have been deposited with the Cambridge Crystallographic Data Centre, CCDC, 12 Union Road, Cambridge CB21EZ, UK. Copies of the data can be obtained free of charge on quoting the depository numbers CCDC-1970034 for **2a**, CCDC-1970035 for **2b**, CCDC-1970036 for **3a·4a·**LiCl·2Et_2O, and CCDC-1970037 for 5 (Fax: +44-1223-336-033; E-Mail: deposit@ccdc.cam.ac.uk, http://www.ccdc.cam.ac.uk)

Supporting Information (see footnote on the first page of this article): NMR spectra, NMR spectroscopic monitoring of the decay, and details to the crystal data and structure refinement procedures

Acknowledgements

We acknowledge the valuable support of the NMR (www.nmr.uni-jena.de/) and mass spectrometry service platforms (www.ms.uni-jena.de/) of the Faculty of Chemistry and Earth Sciences of the Friedrich Schiller University Jena, Germany. Open access funding enabled and organized by Projekt DEAL.

Keywords: Phosphanides; Lithium; Potassium; Phosphanidylphosphane oxides; Mechanistic study

References

[1] a) K. B. Dillon, F. Mathey, J. F. Nixon: *Phosphorus: The Carbon Copy – From Organophosphorus to Phospha-organic Chemistry*, Wiley, Chichester, **1998**; b) M. C. Simpson, J. D. Protasiewicz, *Pure Appl. Chem.* **2013**, *85*, 801–815.

[2] a) K. Issleib, B. Walther, *Angew. Chem. Int. Ed. Engl.* **1967**, *6*, 88–89; b) K. Issleib, B. Walther, *J. Organomet. Chem.* **1970**, *22*, 375–386. See also e.g.: V. P. Morgalyuk, T. V. Strelkova, E. E. Nifant'ev, V. K. Brel, *Mendeleev Commun.* **2016**, *26*, 397–398; V. P. Morgalyuk, T. V. Strelkova, E. E. Nifant'ev, V. K. Brel, *Phosphorus Sulfur Silicon Relat. Elem.* **2016**, *191*, 1462–1463.

[3] Recent reviews: a) Z. Fei, P. J. Dyson, *Coord. Chem. Rev.* **2005**, *249*, 2056–2074; b) M. Alajarín, C. López-Leonardo, P. Llamas-Lorente, *Top. Curr. Chem.* **2005**, *250*, 77–106; c) C. A. Kumar, T. K. Panda, *Phosphorus Sulfur Silicon Relat. Elem.* **2017**, *192*, 1084–1101; d) E. V. Goud, A. Sivaramakrishna, K. Vijayakrishna, *Top. Curr. Chem.* **2017**, *375*, 10.
[4] a) J. McKechnie, D. S. Payne, W. Sim, *J. Chem. Soc.* **1965**, 3500–3501; b) S. Inokawa, Y. Tanaka, H. Yoshida, T. Ogata, *Chem. Lett.* **1972**, *1*, 469–470; c) V. L. Foss, Y. A. Veits, I. F. Lutsenko, *Phosphorus Sulfur* **1977**, *3*, 299–307; d) V. L. Foss, V. A. Solodenko, I. F. Lutsenko, *Zh. Obshchei Khim.* **1979**, *49*, 2418–2428; e) D. Hunter, J. K. Michie, J. A. Miller, W. Stewart, *Phosphorus Sulfur* **1981**, *10*, 267–270.
[5] Y. Sato, S.-i. Kawaguchi, A. Nomoto, A. Ogawa, *Angew. Chem. Int. Ed.* **2016**, *55*, 9700–9703.
[6] I. F. Lutsenko, V. L. Foss, *Pure Appl. Chem.* **1980**, *52*, 917–944.
[7] D. Dhara, P. Kalita, S. Mondal, R. S. Narayanan, K. R. Mote, V. Huch, M. Zimmer, C. B. Yildiz, D. Scheschkewitz, V. Chandrasekhar, A. Jana, *Chem. Sci.* **2018**, *9*, 4235–4243.
[8] a) T. Chen, L.-B. Han, *Synlett* **2015**, *26*, 1153–1163; b) J.-L. Montchamp, *Acc. Chem. Res.* **2014**, *47*, 77–87; c) J.-L. Montchamp, *Pure Appl. Chem.* **2019**, *91*, 113–120.
[9] H.-P. Abicht, K. Issleib, *Z. Anorg. Allg. Chem.* **1978**, *447*, 53–63.
[10] a) J. Kallmerten, M. D. Wittman, *Tetrahedron Lett.* **1986**, *27*, 2443–2446; b) K. M. Brown, N. J. Lawrence, J. Liddle, F. Muhammad, D. A. Jackson, *Tetrahedron Lett.* **1994**, *35*, 6733–6736; c) E. Vedejs, J. A. Garcia-Rivas, *J. Org. Chem.* **1994**, *59*, 6517–6518.
[11] M. Al-Shabatat, P. Schüler, S. Krieck, H. Görls, M. Westerhausen, *Z. Anorg. Allg. Chem.* **2018**, *644*, 1274–1279. See also: Z. Garcá-Hernández, A. Flores-Parra, J. M. Grevy, Á. Ramos-Organillo, R. Contreras, *Polyhedron* **2006**, *25*, 1662–1672.
[12] a) V. Gutmann, G. Mörtl, K. Utvary, *Monatsh. Chem.* **1963**, *94*, 897–903; b) D. J. Birdsall, J. Green, T. Q. Ly, J. Novosad, M. Necas, A. M. Z. Slawin, J. D. Woollins, Z. Zak, *Eur. J. Inorg. Chem.* **1999**, 1445–1452; c) S. J. Coles, S. H. Dale, M. R. J. Elsegood, K. G. Gaw, T. Gelbrich, M. B. Hursthouse, M. E. Light, T. A. Noble, M. B. Smith, *Eur. J. Inorg. Chem.* **2012**, 859–865; d) K. Naktode, R. K. Kottalanka, S. K. Jana, T. K. Panda, *Z. Anorg. Allg. Chem.* **2013**, *639*, 999–1003; e) R. K. Kottalanka, K. Naktode, T. K. Panda, *J. Mol. Struct.* **2013**, *1036*, 188–195; f) R. K. Kottalanka, K. Naktode, S. Anga, H. P. Nayek, T. K. Panda, *Dalton Trans.* **2013**, *42*, 4947–4956; g) N. S. Kariaka, V. A. Trush, T. Y. Sliva, V. V. Dyakonenko, O. V. Shishkin, V. A. Amirkhanov, *J. Mol. Struct.* **2014**, *1068*, 71–76.
[13] a) A. Schmidpeter, S. Lochschmidt, G. Burget, W. S. Sheldrick, *Phosphorus Sulfur* **1983**, *18*, 23–26; b) A. Schmidpeter, G. Burget, *Z. Naturforsch. B* **1985**, *40*, 1306–1313.
[14] A. Schmidpeter, G. Burget, H. G. von Schnering, D. Weber, *Angew. Chem. Int. Ed. Engl.* **1984**, *23*, 816–817.
[15] a) J. D. Protasiewicz, *Eur. J. Inorg. Chem.* **2012**, 4539–4549; b) R. Waterman, *Chemistry* **2016**, *1*, 27–29; c) L. Dostal, *Coord. Chem. Rev.* **2017**, *353*, 142–158.
[16] a) S. Shah, J. D. Protasiewicz, *Chem. Commun.* **1998**, 1585–1586; b) E. Urnezius, S. Shah, J. D. Protasiewicz, *Phosphorus Sulfur Silicon Relat. Elem.* **1999**, *144–146*, 137–139.
[17] P. Le Floch, F. Mathey, *Synlett* **1990**, 171–172.
[18] a) L. Weber, *Eur. J. Inorg. Chem.* **2007**, 4095–4117; b) T. Krachko, J. C. Slootweg, *Eur. J. Inorg. Chem.* **2018**, 2734–2754.
[19] Recent reviews: a) G. Huttner, *Pure Appl. Chem.* **1986**, *58*, 585–596; b) G. Huttner, K. Evertz, *Acc. Chem. Res.* **1986**, *19*, 406–413; c) F. Mathey, *Angew. Chem. Int. Ed. Engl.* **1987**, *26*, 275–286; d) A. H. Cowley, *Acc. Chem. Res.* **1997**, *30*, 445–451; e) F. Mathey, N. H. T. Huy, A. Marinetti, *Helv. Chim. Acta* **2001**, *84*, 2938–2957; f) A. D. Hopkins, J. A. Wood, D. S. Wright, *Coord. Chem. Rev.* **2001**, *216–217*, 155–172; g) K. Lammertsma, M. J. M. Vlaar, *Eur. J. Org. Chem.* **2002**, 1127–1138; h) K. Lammertsma, *Top. Curr. Chem.* **2003**, *229*, 95–119; i) F. Mathey, *Dalton Trans.* **2007**, 1861–1868; j) B. D. Ellis, C. L. B. Macdonald, *Coord. Chem. Rev.* **2007**, *251*, 936–973; k) R. Waterman, *Dalton Trans.* **2009**, 18–26; l) H. Aktas, J. C. Slootweg, K. Lammertsma, *Angew. Chem. Int. Ed.* **2010**, *49*, 2102–2113; m) Y. Hao, D. Wu, R. Tian, Z. Duan, F. Mathey, *Dalton Trans.* **2016**, *45*, 891–893; n) F. Mathey, Z. Duan, *Dalton Trans.* **2016**, *45*, 1804–1809; o) M. E. García, D. García-Vivó, A. Ramos, M. A. Ruiz, *Coord. Chem. Rev.* **2017**, *330*, 1–36.
[20] M. A. Beswick, N. L. Cromhout, C. N. Harmer, J. S. Palmer, P. R. Raithby, A. Steiner, K. L. Verhorevoort, D. S. Wright, *Chem. Commun.* **1997**, 583–584.
[21] F. Pauer, P. P. Power in A.-M. Sapse, P. v. R. Schleyer (Eds.), *Lithium Chemistry: A Theoretical and Experimental Overview*, Wiley, New York, **1995**; ch. 9, pp. 295–392.
[22] R. A. Bartlett, M. M. Olmstead, P. P. Power, G. A. Sigel, *Inorg. Chem.* **1987**, *26*, 1941–1946.
[23] K. Niediek, B. Neumüller, *Z. Anorg. Allg. Chem.* **1993**, *619*, 885–888.
[24] G. W. Rabe, I. A. Guzei, A. L. Rheingold, *Inorg. Chim. Acta* **2001**, *315*, 254–257.
[25] a) K. Fromm, private communication, CSD data base QEDZOO, **2000**; b) M. Nieger, E. Niecke, D. Schmidt, private communication, CSD data base QEDZOO01, **2009**.
[26] C. Frenzel, F. Somoza, S. Blaurock, E. Hey-Hawkins, *J. Chem. Soc., Dalton Trans.* **2001**, 3115–3118.
[27] C. Frenzel, P. Jörchel, E. Hey-Hawkins, *Chem. Commun.* **1998**, 1363–1364.
[28] I. Jevtovikj, R. Herrero, B. Gómez-Ruiz, P. Lönnecke, E. Hey-Hawkins, *Inorg. Chem.* **2013**, *52*, 4488–4493.
[29] a) G. W. Rabe, S. Kheradmandan, G. P. A. Yap, *Inorg. Chem.* **1998**, *37*, 6541–6543; b) S. T. Liddle, P. L. Arnold, *Dalton Trans.* **2007**, 3305–3313.
[30] G. W. Rabe, H. Heise, L. M. Liable-Sands, I. A. Guzei, A. L. Rheingold, *J. Chem. Soc., Dalton Trans.* **2000**, 1863–1866.
[31] a) S. Kurz, H. Oesen, J. Sieler, E. Hey-Hawkins, *Phosphorus Sulfur Silicon Relat. Elem.* **1996**, *117*, 189–196; b) L. Mokhtabad Amrei, P. W. Dibble, R. T. Boeré, *Can. J. Chem.* **2016**, *94*, 392–400.
[32] a) F. E. Hahn, S. Rupprecht, *Z. Naturforsch. B* **1991**, *46*, 143–146; b) F. Blasberg, M. Bolte, M. Wagner, H.-W. Lerner, *Organometallics* **2012**, *31*, 1001–1005. For a review on coordination chemistry of lithium halides see: R. Snaith, D. S. Wright, in *Lithium Chemistry: A Theoretical and Experimental Overview* (Eds.: A.-M. Sapse, P. v. R. Schleyer), Wiley, New York, Chichester,**1995**, ch. 8, pp. 227–293.
[33] A. J. Hoskin, D. W. Stephan, *Organometallics* **1999**, *18*, 2479–2483.
[34] a) S. M. Härling, H. Görls, S. Krieck, M. Westerhausen, *Inorg. Chem.* **2016**, *55*, 10741–10750; b) S. M. Härling, S. Krieck, H. Görls, M. Westerhausen, *Inorg. Chem.* **2017**, *56*, 9255–9263.
[35] Selected reviews: a) L. Weber, *Chem. Rev.* **1992**, *92*, 1839–1906; b) M. Yoshifuji, *Bull. Chem. Soc. Jpn.* **1997**, *70*, 2881–2893; c) P. P. Power, *Chem. Rev.* **1999**, *99*, 3463–3503; d) M. Yoshifuji, S. Ito, *Top. Curr. Chem.* **2003**, *223*, 67–89; e) Y. Wang, G. H. Robinson, *Chem. Commun.* **2009**, 5201–5213; f) R. C. Fischer, P. P. Power, *Chem. Rev.* **2010**, *110*, 3877–3923; g) M. Yoshifuji, *Eur. J. Inorg. Chem.* **2016**, 607–615.
[36] S. Härling, J. Greiser, T. M. A. Al-Shboul, H. Görls, S. Krieck, M. Westerhausen, *Aust. J. Chem.* **2013**, *66*, 1264–1273.
[37] A. J. Veinot, K. Ramgoolam, N. A. Giffin, J. D. Masuda, *Molbank* **2017**, *2017*, M957.
[38] K. Esfandiarfard, A. I. Arkhypchuk, A. Orthaber, S. Ott, *Dalton Trans.* **2016**, *45*, 2201–2207.
[39] R. K. Haynes, W. W.-L. Lam, I. D. Williams, L.-L. Yeung, *Chem. Eur. J.* **1997**, *3*, 2052–2057.
[40] For comparison see $Ph_2P(O)–O–P(O)Ph_2$, $\delta(^{31}P)$ = +28.2 ppm: E. Lindner, H. Kern, *Z. Naturforsch. B* **1983**, *38*, 790–792.
[41] a) F. Zurmühlen, M. Regitz, *Angew. Chem. Int. Ed. Engl.* **1987**, *26*, 83–84; b) F. Zurmühlen, M. Regitz, *New J. Chem.* **1989**, *13*, 335–340.
[42] D. Bevern, S. Krieck, M. Westerhausen, unpublished results.

[43] G. R. Fulmer, A. J. M. Miller, N. H. Sherden, H. E. Gottlieb, A. Nudelman, B. M. Stoltz, J. E. Bercaw, K. I. Goldberg, *Organometallics* **2010**, *29*, 2176–2179.
[44] P. Kölle, G. Linti, H. Nöth, G. L. Wood, C. K. Narula, R. T. Paine, *Chem. Ber.* **1988**, *121*, 871–879.
[45] E. Hey-Hawkins, S. Kurz, *Z. Naturforsch. B* **1995**, *50*, 239–242.
[46] R. Hooft: COLLECT, Data Collection Software; Nonius B. V., Netherlands, **1998**.
[47] Z. Otwinowski, W. Minor, in *Methods in Enzymology*, vol. *276*, *Macromolecular Crystallography, Part A*, (Eds.: C. W. Carter, R. M. Sweet): pp. 307–326, Academic Press: New York, **1997**.
[48] a) SADABS 2.10, Bruker-AXS Inc., **2002**, Madison, WI, USA; b) L. Krause, R. Herbst-Irmer, G. M. Sheldrick, D. Stalke, *J. Appl. Crystallogr.* **2015**, *48*, 3–10.
[49] G. M. Sheldrick, *Acta Crystallogr., Sect. A* **2008**, *64*, 112–122.
[50] G. M. Sheldrick, *Acta Crystallogr., Sect. C* **2015**, *71*, 3–8.
[51] XP, Siemens Analytical X-ray Instruments Inc., Karlsruhe, Germany, **1990**; Madison, WI, USA, **1994**.

Received: December 9, 2019
Published Online: February 4, 2020

